

## Chapter 6

# Atoms and Spectral Features

Some sections incomplete or unwritten.

From atomic, as opposed to molecular, interactions with light, there are two main types of features in quasar spectra. These are absorption lines from bound-bound transitions, and ionization edges.

### 6.1 Atomic Structure and Nomenclature

Not yet written.

### 6.2 Astrophysical Abundances

Not yet written.

### 6.3 Ionization

The probability of ionization is photon energy dependent. A photon with energy,  $E_\gamma$ , identical to the electron ionization potential,  $\Phi$ , will liberate an electron into the gas with no kinetic energy; there is no energy added to the gas. As the photon energy increases above the electron ionization potential, the probability of ionization decreases as  $(\Phi/E_\gamma)^3$ , and the liberated electron deposits a kinetic energy of

$$K.E. = \frac{1}{2}mv^2 = E_\gamma - \Phi \quad (6.1)$$

into the gas. The cross section per atom for ionization can be written

$$\sigma_\lambda = \sigma_o \left( \frac{\lambda}{\lambda_o} \right)^3 \quad \text{atom cm}^{-2}, \quad (6.2)$$

where  $\sigma_o$  is the cross section at  $E_\gamma = \Phi$ , and  $\lambda_o = hc/\Phi$  is the wavelength of the ionization “edge”. Similarly, in terms of photon frequency, we have

$$\sigma_\nu = \sigma_o \left( \frac{\nu}{\nu_o} \right)^{-3} \quad \text{atom cm}^{-2}. \quad (6.3)$$

where  $\nu_o = \Phi/h$  is the frequency of the ionization edge.

The optical depth is

$$\tau_\lambda = N\sigma_\lambda = N \left( \frac{\lambda}{\lambda_o} \right)^3, \quad (6.4)$$

where  $N$  is the column density.

### 6.3.1 The Lyman Limit Break

In practice, the Ly  $\alpha$  ( $n = 1 \rightarrow n = \infty$ ) ionization for neutral hydrogen, H I, is often seen in quasar spectra. The feature is often called the Lyman limit break because of the sudden break in the continuum flux level at wavelengths below the ionization edge.

The ionization potential for H I is  $\Phi = h\nu_o = 13.6$  eV, corresponding to  $\lambda_o = 912$  Å in the rest-frame of the absorbing gas. A system with a Lyman limit break is often referred to as a Lyman limit system (LSS). At the Lyman limit,  $\sigma_{LL} \simeq 6 \times 10^{-18}$  [cm<sup>-2</sup>], giving

$$\tau_{LL}(\lambda) = \frac{N(\text{H I})}{1.6 \times 10^{17}} \left( \frac{\lambda}{912} \right)^3 \quad \lambda \leq 912 \text{ Å} \quad (6.5)$$

In Fig. 6.1, four LLS are plotted, with  $N(\text{H I})$ , increasing from the lower panel to the upper panel. An  $N(\text{H I})$  of  $10^{17.2}$  cm<sup>-2</sup> corresponds to unity optical depth. At this column density, the LL break is only partial, in that it is not opaque. In the cases of partial LL breaks, one can invert Eq. 6.5 and determine the H I column density directly from the spectral data, independent of velocity structure and thermal broadening ( $b$  parameter).

## 6.4 Energy Levels and Grotrian Diagrams

Not yet written.

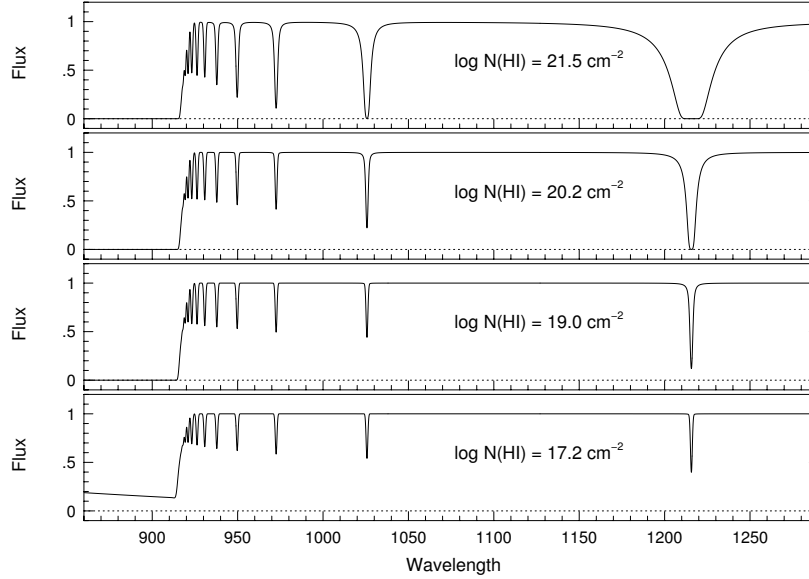


Figure 6.1: — Example of four Lyman limit systems (LLS) in order of increasing H I column density from bottom to top. Note that the break for the lowest column density system is not opaque. This is called a “partial break”. The unsaturated nature of partial breaks make them extremely useful for measuring H I column density.

## 6.5 Common Absorption Lines

Not complete.

We have discussed in some detail the formation of absorption and emission lines in the above sections. The ultimate goal of spectroscopy is to measure the physical quantities that give rise to the absorption. These are the column density,  $N$ , and the  $b$  parameter, which is related to the thermal and/or turbulent properties of the gas. A most powerful technique is to fit the spectral features with Voigt profile in order to directly deduce these physical quantities. However, the data are not always well-suited for Voigt profile analysis. Here, we discuss the equivalent width and the curve of growth, and relate them to  $N$  and  $b$ .

## 6.6 Equivalent Widths

The general definition of the equivalent width is

$$W = \int_{-\infty}^{\infty} \left( 1 - \frac{I_{\lambda}}{I_{\lambda}^o} \right) d\lambda. \quad (6.6)$$

The units of  $W$  are wavelength units, such as Å. The equivalent width represents the width in wavelength of an absorption feature with  $I_{\lambda} = 0$  across the profile (an inverted top hat function) with the identical amount of flux removed from the photon beam. It is also a conserved quantity in that it is independent of the line shape and the resolution of the spectrograph (see below).

Recall that the shape of an absorption profile is given by

$$I_{\lambda} = I_{\lambda}^o \exp(-\tau_{\lambda}) = I_{\lambda}^o \exp[-N\alpha(\lambda)]. \quad (6.7)$$

Rewriting Eq. 6.6 by substituting Eq. 6.7, we have

$$W = \int_{-\infty}^{\infty} [1 - \exp(-\tau_{\lambda})] d\lambda. \quad (6.8)$$

A schematic illustrating the interpretation of the equivalent width is shown in Figure 6.2 for  $W = 0.21$  Å. The integral of the flux remove from the incident light beam is identical for each of the very different absorption profiles. The shaded grey area is the “equivalent profile” with zero flux. The width of this “equivalent profile” is the equivalent width.

As can be seen in Figure 6.2, there can be a family of  $N\alpha(\lambda)$  combinations for fixed  $W$ . That is, the equivalent width is degenerate for various combinations of column density,  $N$ , and absorption coefficient,  $\alpha(\lambda)$ . For a given atomic transition, the shape of  $\alpha(\lambda)$  is governed by  $\Delta\lambda_D$  of the Gaussian component to the Voigt function (see Eq. 5.56). Recall that  $\Delta\lambda_D$  is proportional to the Doppler  $b$  parameter, which is used to characterize the thermal and/or turbulent component to the line broadening.

## 6.7 The Curve of Growth

As shown above, the equivalent width is related to  $N$  and  $b$  through the optical depth,  $\tau_{\lambda} = N\alpha(\lambda)$ . The behavior of the equivalent width dependence on  $N$  and  $b$  is called the curve of growth, or COG. As the optical depth of the line increases, the equivalent width also increases, however the precise functional dependence is sensitive to the optical depth at the line core,  $\tau_o$ .

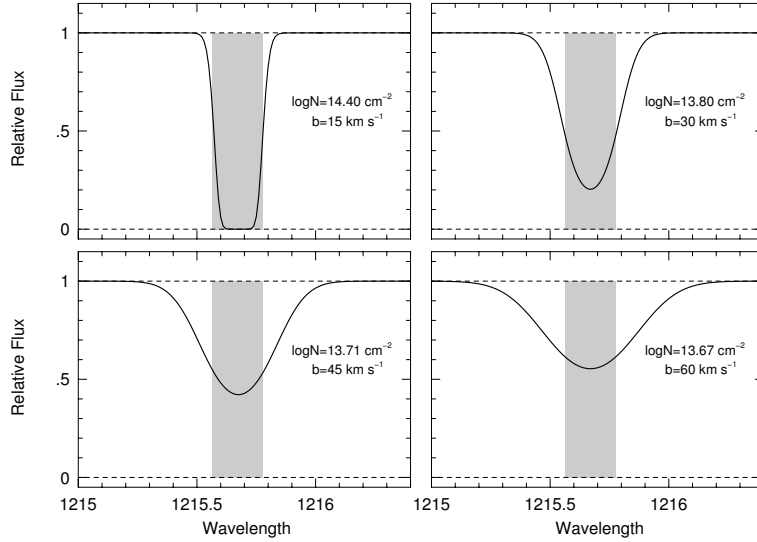


Figure 6.2: — A schematic of four absorptions lines each with equivalent width  $W = 0.21 \text{ \AA}$ . Though the line profile shapes are quite different, the total amount of flux absorbed, as given by Eq. 6.8, are identical. The shaded grey area shows the interpretation of the equivalent width.

As  $\tau_o$  increases, the line depth increases until all the photons at the line core are removed from the incoming beam. At this point, the absorption line is considered to be “saturated”. As  $\tau_o$  increases further, very little additional light is removed from the beam until a regime in which damping wings form at very large  $\tau_o$ . At these large  $\tau_o$  values, the majority of the light is removed far from line center. These three regimes of behavior are called the “linear”, “flat”, and “damped” parts of the COG respectively. These are often referred to as the linear, logarithmic, and square root regimes of the curve of growth due to the functional dependence upon the column density,  $N$ . Note that only in the logarithmic part will  $W$  be sensitive to the  $b$  parameter, and thus the Gaussian component of the line broadening.

In the following sections, the functional dependence of the COG will be examined in detail. For regime of behavior along the COG, a dominant physical process is at play, and this will guide the derivation of  $\tau_o$  for each of the three parts of the COG. In short, we have

$$W \propto N \quad \tau_o \ll 1 \quad \tau_o = \frac{\pi e^2}{mc^2} \lambda^2 N f$$

$$W \propto b\sqrt{\ln(N/b)} \quad 10 \leq \tau_o \leq 10^3 \quad \tau_o = \frac{\pi^{1/2}e^2}{mc} \frac{\lambda}{b} Nf \quad (6.9)$$

$$W \propto \sqrt{N} \quad \tau_o \geq 10^4 \quad \tau_o = \frac{1}{4} \frac{e^2 \Gamma}{mc^3} \lambda^4 Nf$$

In Figure 6.3, the COG for the Ly $\alpha$  ( $n = 1 \rightarrow 2$ ) transition of H I is shown for  $b = 30 \text{ km s}^{-1}$  as a function of  $\tau_o$ . The thick portions of the curves correspond to the flat, logarithmic, and square root parts of the COG, based upon the slope of the curve on a log-log diagram. Insets show the Ly $\alpha$  absorption profiles for locations on the COG, marked with filled circles, in each regime with increasing  $\tau_o$ .

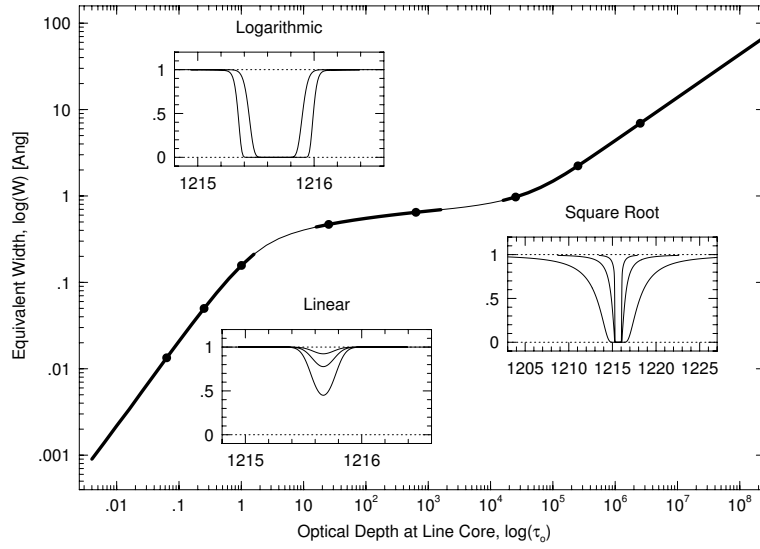


Figure 6.3: — The COG showing the logarithm of equivalent width as a function of the logarithm of the optical depth at line core,  $\tau_o$ , for Ly $\alpha$  for  $b = 30 \text{ km s}^{-1}$ . The three regimes, “linear”, “logarithmic”, and “square root”, corresponding to Eq. 6.10, are shown by the thick curves, respectively, as  $\tau_o$  increases. Absorption profiles are shown for each regime and their locations on the COG marked with filled points. Note the expanded wavelength scale for the profiles on the square root part of the COG. This is due to large damping wings.

### 6.7.1 The Linear Regime

In the optically thin regime, the optical depth in the line core is small,  $\tau_o \ll 1$ . Using series expansion of the exponential, we can approximate

$\exp(-\tau_\lambda) \simeq -\tau_\lambda$ . Substituting into Eq. 6.8, gives

$$W = \int_{-\infty}^{\infty} \tau_\lambda d\lambda = N \int_{-\infty}^{\infty} \alpha(\lambda) d\lambda \quad (6.10)$$

Substituting Eq. 5.56 for  $\alpha(\lambda)$ , we have

$$W = \frac{\pi e^2}{mc} \frac{\lambda^2}{c} N f \int_{-\infty}^{\infty} u(x, y) d\lambda = \tau_o \int_{-\infty}^{\infty} u(x, y) d\lambda, \quad (6.11)$$

which defines  $\tau_o$ , where  $u(x, y)$  is the Voigt function given by Eq. 5.58. By definition the Voigt function has unity normalization, so the integral in Eq. 6.11 equals unity and we have the linear functional dependence,  $W \propto N$ ,

$$W = \frac{\pi e^2}{mc} \frac{\lambda^2}{c} N f. \quad (6.12)$$

Note that the shape of  $u(x, y)$  depends upon the Doppler width,  $\Delta\lambda_D \propto b$ , and is thus dependent upon the gas temperature. However,  $W$  is an integrated quantity and, because the Voigt function has unity normalization, is independent of  $b$  in the regime of  $\tau_o \ll 1$ .

Physically, in the regime of small  $\tau_o$ , as more atoms are added to the absorbing gas,  $W$  grows by a deepening of the line core due to the removal of additional photons in the beam.

### 6.7.2 The Logarithmic Regime

In the regime where  $10 \leq \tau_o \leq 10^3$ , the damping wings of the Lorentzian are insignificant compared to those of the Gaussian contribution, and we can treat the Lorentzian contribution to the absorption coefficient as a  $\delta$  function. We can write the optical depth as

$$\tau_\lambda = N\alpha(\lambda) \simeq \frac{\pi e^2 \lambda^2}{mc^2} N f \frac{1}{\pi^{1/2} \Delta\lambda_D} \exp \left[ - \left( \frac{\Delta\lambda}{\Delta\lambda_D} \right)^2 \right]. \quad (6.13)$$

Defining  $\tau_o = (\pi e^2 \lambda^2 / mc^2) (1/\pi^{1/2} \Delta\lambda_D) N f$ , the optical depth of the line core, and invoking  $x = (\Delta\lambda / \Delta\lambda_D)$ , we can simplify the above equation to

$$\tau_\lambda = \tau_o \exp(-x^2). \quad (6.14)$$

From Eq. 6.8, the equivalent width is then

$$W = \Delta\lambda_D \int_{-\infty}^{\infty} [1 - \exp(-\tau_o e^{-x^2})] dx = \Delta\lambda_D F(\tau_o) \quad (6.15)$$

where

$$F(\tau_o) = \int_{-\infty}^{\infty} [1 - \exp(-\tau_o e^{-x^2})] dx \quad (6.16)$$

$$= \frac{\pi^{1/2}}{2} \sum_{n=1}^{\infty} \frac{(-1)^{n-1} \tau_o^n}{n! n^{1/2}}. \quad (6.17)$$

In the “flat” part of the curve of growth, the line core is saturated, meaning that  $W$  does not grow due to removal of photons with small  $x$ , where the Lorentzian dominates. The function  $F(\tau_o)$  provides the behavior of the line absorption strength in the regime where the width of the line is governed by a Gaussian broadening mechanism. As  $\tau_o$  is increased, the amplitude of the Gaussian increases and the wings of the line remove more flux from the beam. Physically, as more atoms are added to the gas, it is those in the tails of the Doppler velocity distribution that contribute to increasing  $W$ . Thus, as we shall see below,  $W \propto b$  for a fixed  $N$ .

For small  $\tau_o$ , a series expansion of Eq. 6.14 yields Eq. 6.12 for the linear part of the curve of growth. When  $\tau_o$  is large, series expansion yields the asymptotic solution

$$F(\tau_o) = (\ln \tau_o)^{1/2}, \quad (6.18)$$

which gives

$$W = \Delta \lambda_D (\ln \tau_o)^{1/2}. \quad (6.19)$$

From Eq 5.60,  $b = (c/\lambda)\Delta \lambda_D$ , and we have the full form of  $W$  written as

$$W = b \frac{\lambda}{c} \left( \ln \left[ \frac{\pi^{1/2} e^2 \lambda}{mc} \frac{\lambda}{b} N f \right] \right)^{1/2}. \quad (6.20)$$

### 6.7.3 The Square Root Regime

In this regime, where  $\tau_o > 10^4$ , the Lorentzian dominates due to very strong and broad wings. In this case, the Gaussian contribution to the Voigt function can be treated as if it were a  $\delta$  function. Thus, we can write the optical depth as

$$\tau_\lambda = N \alpha(\lambda) \simeq \frac{\pi e^2 \lambda^2}{mc^2} N f \frac{\Gamma \lambda^2 / 4\pi c}{(\Delta \lambda)^2 + (\Gamma \lambda^2 / 4\pi c)^2} \quad (6.21)$$

where  $\alpha(\lambda)$  is given by Eq. 5.17. Defining  $\beta = \Gamma \lambda^2 / 4\pi c^2$ , we rewrite this as

$$\tau_\lambda = \frac{\pi e^2 \lambda^2}{mc^2} N f \frac{\beta}{(\Delta \lambda)^2 + \beta^2} \quad (6.22)$$



Due to the behavior of the Lorentzian, the majority of the energy removed from the beam is in wings of the absorption line. Thus, the equivalent width is dominated by regions under the line profile that are far from the line center. Under this assumption,  $\Delta\lambda \gg \beta$ , which leads to the approximation

$$\tau_\lambda = \frac{\pi e^2 \lambda^2}{mc^2} N f \frac{\beta}{(\Delta\lambda)^2} \frac{1}{1 + (\beta/\Delta\lambda)^2} \simeq \frac{\tau_o}{(\Delta\lambda)^2}, \quad (6.23)$$

where we define  $\tau_o = \beta(\pi e^2 \lambda^2 / (mc^2) N f)$ , the optical depth at the line center. Substituting this into Eq. 6.6, we have

$$W \simeq \int_{-\infty}^{\infty} [1 - \exp(-\tau_o/(\Delta\lambda)^2)] d\lambda. \quad (6.24)$$

The functional dependence of  $W$  can be obtained by a change of variable. Let  $u^2 = (\Delta\lambda)^2/\tau_o$ , then  $du = d\lambda/\sqrt{\tau_o}$ . Substituting onto the above integral, we have

$$W \simeq \tau_o^{1/2} \int_{-\infty}^{\infty} [1 - \exp(-1/u^2)] du = \tau_o^{1/2} F \quad (6.25)$$

where  $F$  is the value of the integral (a Gamma function, but yields a constant because there is no dependence upon  $\tau_o$ ). Writing out  $\tau_o$  fully, we have

$$W \simeq F \frac{\lambda^2}{c^2} \left( \frac{e^2}{4m} \Gamma N f \right)^{1/2}. \quad (6.26)$$

Note that  $W \propto \sqrt{\Gamma N}$ , giving this regime either the name “square root” or “damping” part of the curve of growth.

In Figure 6.4, the COGs are shown for the often observed transitions  $\text{Ly}\alpha$   $\lambda 1215$ ,  $\text{MgII}$   $\lambda 2796$ ,  $\text{CIV}$   $\lambda 1548$ , and  $\text{OVI}$   $\lambda 1031$ . The point of the illustration is that each of the COGs have very similar behavior. The only distinctions are the column density regimes of the three main parts of the COGs. In practice, only the  $\text{Ly}\alpha$  transition is observed on the square root (damping) part of the COG.

However, it can be challenging to deduce the column density in the logarithmic (flat) part of the COG. In this regime, it is necessary to include information from additional transition from the same ionic species.

## 6.8 Rest-Frame Equivalent Widths

When absorption lines are redshifted, the observed equivalent widths increase with the factor  $1 + z$ , where the definition of redshift is

$$z = \frac{\lambda - \lambda_r}{\lambda_r}, \quad (6.27)$$

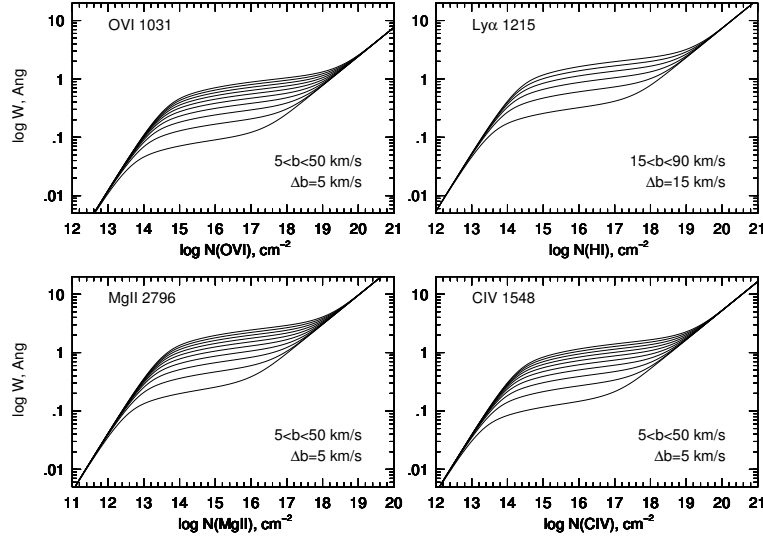


Figure 6.4: — The curve of growth for  $\text{Ly}\alpha$   $\lambda 1215$ ,  $\text{MgII}$   $\lambda 2796$ ,  $\text{CIV}$   $\lambda 1548$ , and  $\text{OVI}$   $\lambda 1031$ . For each species, the logarithm of the equivalent width [ $\text{\AA}$ ] is plotted vs. the logarithm of the column density. For the curves shown, the range of  $b$  parameters are given in the lower right corner of the panels, with  $b$  increasing in steps of  $\Delta b$  upward.

where  $\lambda$  is the observed wavelength of a feature with rest-frame wavelength  $\lambda_r$ . We thus have the well-known relationship

$$\lambda = \lambda_r(1 + z). \quad (6.28)$$

This can easily be shown by considering a idealized absorption line with a top-hat profile with a width  $\Delta\lambda = \lambda_- - \lambda_+$ . This can be expressed by the function

$$I_\lambda = \begin{cases} I_\lambda^c & : \lambda < \lambda_- \\ 0 & : \lambda_- \leq \lambda \leq \lambda_+ \\ I_\lambda^c & : \lambda > \lambda_+. \end{cases} \quad (6.29)$$

The equivalent width in the rest-frame is

$$W_r = \int_{-\infty}^{\infty} \left(1 - \frac{I_\lambda}{I_\lambda^c}\right) d\lambda = \int_{\lambda_-}^{\lambda_+} d\lambda = \Delta\lambda. \quad (6.30)$$

Now, let this absorption line be redshifted by some arbitrary  $z$ . The observed equivalent width is then

$$W = \int_{-\infty}^{\infty} \left(1 - \frac{I_\lambda}{I_\lambda^c}\right) d\lambda = \int_{\lambda_-(1+z)}^{\lambda_+(1+z)} d\lambda = \Delta\lambda(1 + z). \quad (6.31)$$

The relationship between equivalent width and redshift is schematically illustrated in Fig. 6.5 for a Ly $\alpha$  line with  $W_r = 1.0 \text{ \AA}$  redshifted from  $z = 0$  to  $z = 0.5$ . Comparing Eqs 6.30 and 6.31, we have the relationship between an observed redshifted equivalent width and the rest-frame equivalent width,

$$W_r = \frac{W}{1+z}. \quad (6.32)$$

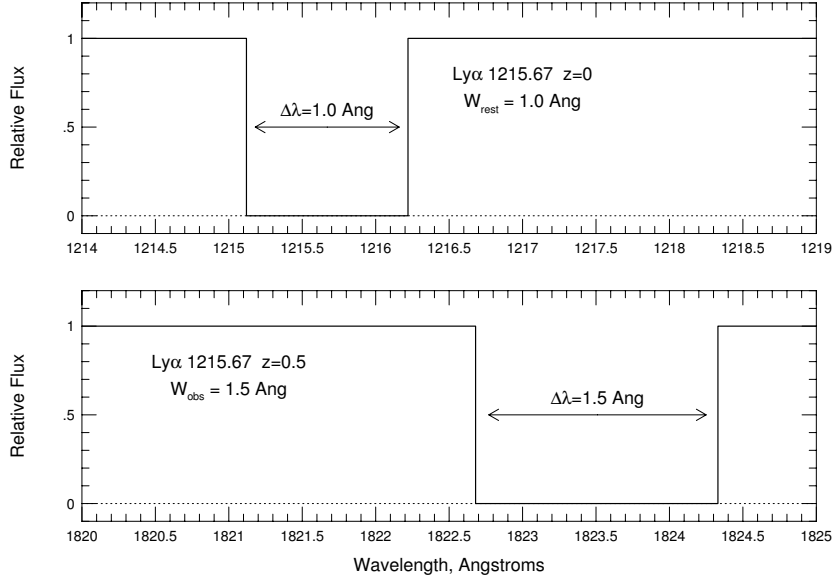


Figure 6.5: — (upper) An idealized Ly $\alpha$   $\lambda$ 1215.67 absorption line, given by Eq. 6.29, at  $z = 0$  with  $W_r = 1.0 \text{ \AA}$ . — (lower) The same idealized profile redshifts to  $z = 0.5$ . The central wavelength and the upper and lower limits of the profile,  $\lambda_-$  and  $\lambda_+$ , are shifted by the factor  $1+z$ . The result is that  $W = W_r(1+z)$ .

As can be seen directly from the above example, the width of an observed absorption line is a factor of  $1+z$  larger than the rest-frame width. All measured absorption properties must always be converted into their rest-frame before any analysis. An important consequence of Eq. 6.32, is that the rest-frame equivalent width threshold of a survey actually improves with increasing redshift, assuming a fairly uniform signal-to-noise ratio with wavelength in the spectra.

